

Search For Charged Higgs Decays of the Top Quark Using Hadronic Decays of the Tau Lepton

F. Abe,¹⁷ H. Akimoto,³⁶ A. Akopian,³¹ M. G. Albrow,⁷ S. R. Amendolia,²⁷ D. Amidei,²⁰ J. Antos,³³ S. Aota,³⁶ G. Apollinari,³¹ T. Asakawa,³⁶ W. Ashmanskas,¹⁸ M. Atac,⁷ F. Azfar,²⁶ P. Azzi-Bacchetta,²⁵ N. Bacchetta,²⁵ W. Badgett,²⁰ S. Bagdasarov,³¹ M. W. Bailey,²² J. Bao,³⁹ P. de Barbaro,³⁰ A. Barbaro-Galtieri,¹⁸ V. E. Barnes,²⁹ B. A. Barnett,¹⁵ M. Barone,⁹ E. Barzi,⁹ G. Bauer,¹⁹ T. Baumann,¹¹ F. Bedeschi,²⁷ S. Behrends,³ S. Belforte,²⁷ G. Bellettini,²⁷ J. Bellinger,³⁸ D. Benjamin,³⁵ J. Benlloch,¹⁹ J. Bensinger,³ D. Benton,²⁶ A. Beretvas,⁷ J. P. Berge,⁷ J. Berryhill,⁵ S. Bertolucci,⁹ B. Bevensee,²⁶ A. Bhatti,³¹ K. Biery,⁷ M. Binkley,⁷ D. Bisello,²⁵ R. E. Blair,¹ C. Blocker,³ A. Bodek,³⁰ W. Bokhari,¹⁹ V. Bolognesi,² G. Bolla,²⁹ D. Bortoletto,²⁹ J. Boudreau,²⁸ L. Breccia,² C. Bromberg,²¹ N. Bruner,²² E. Buckley-Geer,⁷ H. S. Budd,³⁰ K. Burkett,²⁰ G. Busetto,²⁵ A. Byon-Wagner,⁷ K. L. Byrum,¹ J. Cammerata,¹⁵ C. Campagnari,⁷ M. Campbell,²⁰ A. Caner,²⁷ W. Carithers,¹⁸ D. Carlsmith,³⁸ A. Castro,²⁵ D. Cauz,²⁷ Y. Cen,³⁰ F. Cervelli,²⁷ P. S. Chang,³³ P. T. Chang,³³ H. Y. Chao,³³ J. Chapman,²⁰ M. -T. Cheng,³³ G. Chiarelli,²⁷ T. Chikamatsu,³⁶ C. N. Chiou,³³ L. Christofek,¹³ S. Cihangir,⁷ A. G. Clark,¹⁰ M. Cobal,²⁷ E. Cocca,²⁷ M. Contreras,⁵ J. Conway,³² J. Cooper,⁷ M. Cordelli,⁹ C. Couyoumtzelis,¹⁰ D. Crane,¹ D. Cronin-Hennessy,⁶ R. Culbertson,⁵ T. Daniels,¹⁹ F. DeJongh,⁷ S. Delchamps,⁷ S. Dell'Agnello,²⁷ M. Dell'Orso,²⁷ R. Demina,⁷ L. Demortier,³¹ M. Deninno,² P. F. Derwent,⁷ T. Devlin,³² J. R. Dittmann,⁶ S. Donati,²⁷ J. Done,³⁴ T. Dorigo,²⁵ A. Dunn,²⁰ N. Eddy,²⁰ K. Einsweiler,¹⁸ J. E. Elias,⁷ R. Ely,¹⁸ E. Engels, Jr.,²⁸ D. Errede,¹³ S. Errede,¹³ Q. Fan,³⁰ G. Feild,³⁹ C. Ferretti,²⁷ I. Fiori,² B. Flaugher,⁷ G. W. Foster,⁷ M. Franklin,¹¹ M. Frautschi,³⁵ J. Freeman,⁷ J. Friedman,¹⁹ H. Frisch,⁵ Y. Fukui,¹⁷ S. Funaki,³⁶ S. Galeotti,²⁷ M. Gallinaro,²⁶ O. Ganel,³⁵ M. Garcia-Sciveres,¹⁸ A. F. Garfinkel,²⁹ C. Gay,¹¹ S. Geer,⁷ D. W. Gerdes,¹⁵ P. Giannetti,²⁷ N. Giokaris,³¹ P. Giromini,⁹ G. Giusti,²⁷ L. Gladney,²⁶ D. Glenzinski,¹⁵ M. Gold,²² J. Gonzalez,²⁶ A. Gordon,¹¹ A. T. Goshaw,⁶ Y. Gotra,²⁵ K. Goulios,³¹ H. Grassmann,²⁷ L. Groer,³² C. Grosso-Pilcher,⁵ G. Guillian,²⁰ R. S. Guo,³³ C. Haber,¹⁸ E. Hafen,¹⁹ S. R. Hahn,⁷ R. Hamilton,¹¹ R. Handler,³⁸ R. M. Hans,³⁹ F. Happacher,⁹ K. Hara,³⁶ A. D. Hardman,²⁹ B. Harral,²⁶ R. M. Harris,⁷ S. A. Hauger,⁶ J. Hauser,⁴ C. Hawk,³² E. Hayashi,³⁶ J. Heinrich,²⁶ B. Hinrichsen,¹⁴ K. D. Hoffman,²⁹ M. Hohlmann,⁵ C. Holck,²⁶ R. Hollebeek,²⁶ L. Holloway,¹³ S. Hong,²⁰ G. Houk,²⁶ P. Hu,²⁸ B. T. Huffman,²⁸ R. Hughes,²³ J. Huston,²¹ J. Huth,¹¹ J. Huyen,⁷ H. Ikeda,³⁶ M. Incagli,²⁷ J. Incandela,⁷ G. Introzzi,²⁷ J. Iwai,³⁶ Y. Iwata,¹² H. Jensen,⁷ U. Joshi,⁷ R. W. Kadel,¹⁸ E. Kajfasz,²⁵ H. Kambara,¹⁰ T. Kamon,³⁴ T. Kaneko,³⁶ K. Karr,³⁷ H. Kasha,³⁹ Y. Kato,²⁴ T. A. Keaffaber,²⁹ K. Kelley,¹⁹ R. D. Kennedy,⁷ R. Kephart,⁷ P. Kesten,¹⁸ D. Kestenbaum,¹¹ H. Keutelian,⁷ F. Keyvan,⁴ B. Kharadia,¹³ B. J. Kim,³⁰ D. H. Kim,^{7*} H. S. Kim,¹⁴ S. B. Kim,²⁰ S. H. Kim,³⁶ Y. K. Kim,¹⁸ L. Kirsch,³ P. Koehn,²³ K. Kondo,³⁶ J. Konigsberg,⁸ S. Kopp,⁵ K. Kordas,¹⁴ A. Korytov,⁸ W. Koska,⁷ E. Kovacs,^{7*} W. Kowald,⁶ M. Krasberg,²⁰ J. Kroll,⁷ M. Kruse,³⁰ T. Kuwabara,³⁶ S. E. Kuhlmann,¹ E. Kuns,³² A. T. Laasanen,²⁹ S. Lami,²⁷ S. Lammel,⁷ J. I. Lamoureux,³ M. Lancaster,¹⁸ T. LeCompte,¹ S. Leone,²⁷ J. D. Lewis,⁷ P. Limon,⁷ M. Lindgren,⁴ T. M. Liss,¹³ J. B. Liu,³⁰ Y. C. Liu,³³ N. Lockyer,²⁶ O. Long,²⁶ C. Loomis,³² M. Loreti,²⁵ J. Lu,³⁴ D. Lucchesi,²⁷ P. Lukens,⁷ S. Lusin,³⁸ J. Lys,¹⁸ K. Maeshima,⁷ A. Maghakian,³¹ P. Maksimovic,¹⁹ M. Mangano,²⁷ J. Mansour,²¹ M. Mariotti,²⁵ J. P. Marriner,⁷ A. Martin,³⁹ J. A. J. Matthews,²² R. Mattingly,¹⁹ P. McIntyre,³⁴ P. Melese,³¹ A. Menzione,²⁷ E. Meschi,²⁷ S. Metzler,²⁶ C. Miao,²⁰ T. Miao,⁷ G. Michail,¹¹ R. Miller,²¹ H. Minato,³⁶ S. Miscetti,⁹ M. Mishina,¹⁷ H. Mitsushio,³⁶ T. Miyamoto,³⁶ S. Miyashita,³⁶ N. Moggi,²⁷ Y. Morita,¹⁷ A. Mukherjee,⁷ T. Muller,¹⁶ P. Murat,²⁷ H. Nakada,³⁶ I. Nakano,³⁶ C. Nelson,⁷ D. Neuberger,¹⁶ C. Newman-Holmes,⁷ C-Y. P. Ngan,¹⁹ M. Ninomiya,³⁶ L. Nodulman,¹ S. H. Oh,⁶ K. E. Ohl,³⁹ T. Ohmoto,¹² T. Ohsugi,¹² R. Oishi,³⁶ M. Okabe,³⁶ T. Okusawa,²⁴ R. Oliveira,²⁶ J. Olsen,³⁸ C. Pagliarone,²⁷ R. Paoletti,²⁷ V. Papadimitriou,³⁵ S. P. Pappas,³⁹ N. Parashar,²⁷ S. Park,⁷ A. Parri,⁹ J. Patrick,⁷ G. Pauletta,²⁷ M. Paulini,¹⁸ A. Perazzo,²⁷ L. Pescara,²⁵ M. D. Peters,¹⁸ T. J. Phillips,⁶ G. Piacentino,²⁷ M. Pillai,³⁰ K. T. Pitts,⁷ R. Plunkett,⁷ L. Pondrom,³⁸ J. Proudfoot,¹ F. Ptohos,¹¹ G. Punzi,²⁷ K. Ragan,¹⁴ D. Reher,¹⁸ A. Ribon,²⁵ F. Rimondi,² L. Ristori,²⁷ W. J. Robertson,⁶ T. Rodrigo,²⁷ S. Rolli,³⁷ J. Romano,⁵ L. Rosenson,¹⁹ R. Roser,¹³ T. Saab,¹⁴ W. K. Sakumoto,³⁰ D. Saltzberg,⁵ A. Sansoni,⁹ L. Santi,²⁷ H. Sato,³⁶ P. Schlabach,⁷ E. E. Schmidt,⁷ M. P. Schmidt,³⁹ A. Scribano,²⁷ S. Segler,⁷ S. Seidel,²² Y. Seiya,³⁶ G. Sganos,¹⁴ M. D. Shapiro,¹⁸ N. M. Shaw,²⁹ Q. Shen,²⁹ P. F. Shepard,²⁸ M. Shimojima,³⁶ M. Shochet,⁵ J. Siegrist,¹⁸ A. Sill,³⁵ P. Sinervo,¹⁴ P. Singh,²⁸ J. Skarha,¹⁵ K. Sliwa,³⁷ F. D. Snider,¹⁵ T. Song,²⁰ J. Spalding,⁷ T. Speer,¹⁰ P. Spicas,¹⁹ F. Spinella,²⁷ M. Spiropulu,¹¹ L. Spiegel,⁷ L. Stanco,²⁵ J. Steele,³⁸ A. Stefanini,²⁷ K. Strahl,¹⁴ J. Strait,⁷ R. Ströhmer,^{7*} D. Stuart,⁷ G. Sullivan,⁵ K. Sumorok,¹⁹ J. Suzuki,³⁶ T. Takada,³⁶ T. Takahashi,²⁴ T. Takano,³⁶ K. Takikawa,³⁶ N. Tamura,¹² B. Tannenbaum,²² F. Tartarelli,²⁷ W. Taylor,¹⁴ P. K. Teng,³³ Y. Teramoto,²⁴ S. Tether,¹⁹ D. Theriot,⁷ T. L. Thomas,²² R. Thun,²⁰ R. Thurman-Keup,¹ M. Timko,³⁷ P. Tipton,³⁰ A. Titov,³¹ S. Tkaczyk,⁷ D. Toback,⁵ K. Tollefson,³⁰ A. Tollestrup,⁷ H. Toyoda,²⁴ W. Trischuk,¹⁴ J. F. de Troconiz,¹¹ S. Truitt,²⁰ J. Tseng,¹⁹ N. Turini,²⁷ T. Uchida,³⁶ N. Uemura,³⁶ F. Ukegawa,²⁶ G. Unal,²⁶ J. Valls,^{7*} S. C. van den Brink,²⁸ S. Vejck, III,²⁰ G. Velez,²⁷ R. Vidal,⁷ R. Vilar,^{7*} M. Vondracek,¹³

D. Vucinic,¹⁹ R. G. Wagner,¹ R. L. Wagner,⁷ J. Wahl,⁵ N. B. Wallace,²⁷ A. M. Walsh,³² C. Wang,⁶ C. H. Wang,³³
 J. Wang,⁵ M. J. Wang,³³ Q. F. Wang,³¹ A. Warburton,¹⁴ T. Watts,³² R. Webb,³⁴ C. Wei,⁶ H. Wenzel,¹⁶
 W. C. Wester, III,⁷ A. B. Wicklund,¹ E. Wicklund,⁷ R. Wilkinson,²⁶ H. H. Williams,²⁶ P. Wilson,⁵ B. L. Winer,²³
 D. Winn,²⁰ D. Wolinski,²⁰ J. Wolinski,²¹ S. Worm,²² X. Wu,¹⁰ J. Wyss,²⁵ A. Yagil,⁷ W. Yao,¹⁸ K. Yasuoka,³⁶
 Y. Ye,¹⁴ G. P. Yeh,⁷ P. Yeh,³³ M. Yin,⁶ J. Yoh,⁷ C. Yosef,²¹ T. Yoshida,²⁴ D. Yovanovitch,⁷ I. Yu,⁷ L. Yu,²²
 J. C. Yun,⁷ A. Zanetti,²⁷ F. Zetti,²⁷ L. Zhang,³⁸ W. Zhang,²⁶ and S. Zucchelli²
 (CDF Collaboration)

- ¹ Argonne National Laboratory, Argonne, Illinois 60439
² Istituto Nazionale di Fisica Nucleare, University of Bologna, I-40127 Bologna, Italy
³ Brandeis University, Waltham, Massachusetts 02264
⁴ University of California at Los Angeles, Los Angeles, California 90024
⁵ University of Chicago, Chicago, Illinois 60638
⁶ Duke University, Durham, North Carolina 28708
⁷ Fermi National Accelerator Laboratory, Batavia, Illinois 60510
⁸ University of Florida, Gainesville, FL 33611
⁹ Laboratori Nazionali di Frascati, Istituto Nazionale di Fisica Nucleare, I-00044 Frascati, Italy
¹⁰ University of Geneva, CH-1211 Geneva 4, Switzerland
¹¹ Harvard University, Cambridge, Massachusetts 02138
¹² Hiroshima University, Higashi-Hiroshima 724, Japan
¹³ University of Illinois, Urbana, Illinois 61801
¹⁴ Institute of Particle Physics, McGill University, Montreal H3A 2T8, and University of Toronto, Toronto M5S 1A7, Canada
¹⁵ The Johns Hopkins University, Baltimore, Maryland 21218
¹⁶ Universitaet Karlsruhe, 76128 Karlsruhe, Germany
¹⁷ National Laboratory for High Energy Physics (KEK), Tsukuba, Ibaraki 315, Japan
¹⁸ Ernest Orlando Lawrence Berkeley National Laboratory, Berkeley, California 94720
¹⁹ Massachusetts Institute of Technology, Cambridge, Massachusetts 02139
²⁰ University of Michigan, Ann Arbor, Michigan 48109
²¹ Michigan State University, East Lansing, Michigan 48824
²² University of New Mexico, Albuquerque, New Mexico 87132
²³ The Ohio State University, Columbus, OH 43320
²⁴ Osaka City University, Osaka 588, Japan
²⁵ Universita di Padova, Istituto Nazionale di Fisica Nucleare, Sezione di Padova, I-36132 Padova, Italy
²⁶ University of Pennsylvania, Philadelphia, Pennsylvania 19104
²⁷ Istituto Nazionale di Fisica Nucleare, University and Scuola Normale Superiore of Pisa, I-56100 Pisa, Italy
²⁸ University of Pittsburgh, Pittsburgh, Pennsylvania 15270
²⁹ Purdue University, West Lafayette, Indiana 47907
³⁰ University of Rochester, Rochester, New York 14628
³¹ Rockefeller University, New York, New York 10021
³² Rutgers University, Piscataway, New Jersey 08854
³³ Academia Sinica, Taipei, Taiwan 11530, Republic of China
³⁴ Texas A&M University, College Station, Texas 77843
³⁵ Texas Tech University, Lubbock, Texas 79409
³⁶ University of Tsukuba, Tsukuba, Ibaraki 315, Japan
³⁷ Tufts University, Medford, Massachusetts 02155
³⁸ University of Wisconsin, Madison, Wisconsin 53806
³⁹ Yale University, New Haven, Connecticut 06511

(August 14, 2018)

This Letter describes a direct search for charged Higgs boson production in $p\bar{p}$ collisions at $\sqrt{s} = 1.8$ TeV recorded by the Collider Detector at Fermilab. Two-Higgs-doublet extensions to the standard model predict the existence of charged Higgs bosons (H^\pm). In such models, the branching fraction for top quarks $\mathcal{B}(t \rightarrow H^+b \rightarrow \tau^+\nu b)$ can be large. This search uses the hadronic decays of the tau lepton in this channel to significantly extend previous limits on H^\pm production.

Many extensions to the standard model (SM), including a large class of supersymmetric models, have an expanded Higgs sector containing two Higgs doublets where one doublet couples to the up-type quarks and neutrinos, and the other couples to the down-type quarks and charged leptons [1]. In these theories, electroweak symmetry breaking produces five Higgs bosons, three of which are neutral and two of which are charged.

Recent searches for charged Higgs bosons (H^\pm) include analyses from $p\bar{p}$ collisions at the $Spp\bar{S}$ [2] and the Tevatron [3,4], from e^+e^- collisions at CESR [5] and at LEP [6], and from world averages of the tau lepton branching ratios. An indirect limit from these averages excludes at 90% confidence level (C.L.) any charged Higgs with $M_{H^\pm} < 1.5 \tan\beta \text{ GeV}/c^2$ [7] where $\tan\beta$ is the ratio of the vacuum expectation values of the two Higgs doublets.

Based on a measurement of the inclusive $b \rightarrow s\gamma$ cross section, CLEO indirectly excludes at 95% C.L. charged Higgs bosons with $M_{H^\pm} \lesssim 244 \text{ GeV}/c^2$ for $\tan\beta \gtrsim 50$, assuming only a two-Higgs-doublet extension to the standard model [5]. Models with a richer particle structure, such as supersymmetry, can evade this limit with compensating destructive interference from particles other than the W and H^\pm [8].

Based on direct searches for charged Higgs pair production, the LEP experiments exclude at 95% C.L. any charged Higgs with a mass lower than $44.1 \text{ GeV}/c^2$ [6].

The Collider Detector at Fermilab (CDF) and DØ have recently established the existence of the top quark via its semileptonic decays [9,10] using $p\bar{p}$ collisions at $\sqrt{s} = 1.8 \text{ TeV}$. In the analysis presented here, we search for $t\bar{t}$ events in which the top quarks decay into charged Higgs bosons. By using a data sample which is five times larger, improved tau lepton identification, and b -quark tagging, this analysis significantly extends the charged Higgs limits from a similar, previous CDF search [3].

CDF is a magnetic spectrometer containing tracking detectors, calorimeters, and muon chambers [11]. The tracking detectors lie inside a 1.4 T solenoidal magnetic field. The central tracking chamber (CTC) measures the momenta of charged particles over a pseudorapidity range $|\eta| < 1.1$ where $\eta \equiv -\ln \tan(\theta/2)$ [12]. A silicon vertex detector, positioned immediately outside the beampipe and inside the CTC, provides precise charged particle reconstruction and allows identification of secondary vertices from b -quark decays [13]. Electromagnetic and hadronic calorimeters, arranged in a projective tower geometry, surround the tracking volume and are used to identify jets, localized clusters of energy, over the range $|\eta| < 4.2$. The presence of neutrinos can be deduced from the missing transverse energy \cancel{E}_T [14].

This analysis relies on data collected with the \cancel{E}_T trigger which nominally requires $\cancel{E}_T > 35 \text{ GeV}$ but is only fully efficient for $\cancel{E}_T \gtrsim 80 \text{ GeV}$. These data, collected from 1992 to 1995, represent an integrated luminosity of

$100 \pm 8 \text{ pb}^{-1}$.

The ratio $\tan\beta$ determines the dominant decay modes for the H^\pm and top quark. We consider only the region $\tan\beta \gtrsim 5$ for which H^\pm decays to $\tau\nu$ exclusively. For $\tan\beta \gtrsim 100$, both top quarks decay via $t \rightarrow Hb$, producing distinctive events with two tau leptons, two b -quarks, and large \cancel{E}_T . For intermediate $\tan\beta$, one or both of the top quarks can decay via $t \rightarrow Wb$, producing events with lower \cancel{E}_T and fewer tau leptons. To separate H^\pm events from background, events in our final sample must have one of the two following final states.

In the first final state (“ τjjX ”), events contain one hadronically-decaying tau lepton, two jets, and one or more additional objects. The other object(s) can be either another lepton (electron, muon, or tau) or jet. At least one of the jets must have associated charged particles that form a displaced vertex indicative of a b -quark decay.

The second final state (“di-tau”) preserves acceptance in the region where the charged Higgs mass approaches the top quark mass. In this case, the b -jet energies fall below the jet E_T requirement, causing events to fail the τjjX requirements. In the di-tau final state, events contain two energetic, hadronically-decaying tau leptons that are not opposite in azimuth ($\Delta\phi_{\tau\tau} < 160^\circ$). To avoid double counting, this category excludes events passing the τjjX requirements.

The electron and muon identification cuts are those used for the top quark search [15]. Identified electrons (muons) must have a minimum E_T ($p_T \cdot c$) of 10 GeV.

An iterative algorithm which uses a fixed cone size of $\Delta R \equiv \sqrt{(\Delta\phi)^2 + (\Delta\eta)^2} = 0.4$ finds jets in the calorimeter [16]. Those jets that contain charged particles that form a displaced secondary vertex [9] are categorized as b -jets. Jets identified for this analysis have a minimum uncorrected E_T of 10 GeV.

Tau lepton identification begins with a jet. The tau lepton candidate must have one or three charged particles in a 10° cone about the jet axis and no additional charged particles in a cone of 30° . For counting the number of associated charged particles, only those with a vertex within 5 cm of the tau vertex and $p_T > 1 \text{ GeV}/c$ are used. In addition, the tau lepton candidate’s tracks must have the correct total charge $Q = \pm 1e$ and its mass M_τ , determined from tracks and electromagnetic calorimeter energy deposits, must be consistent with that of a tau lepton ($M_\tau < 1.8 \text{ GeV}/c^2$). The E_T of the calorimeter cluster associated with the tau lepton candidate must exceed 10 GeV; the largest p_T of an associated charged particle must exceed 10 GeV/ c . The identification algorithm requires $|\eta_\tau| < 1$ to maintain good efficiency for tracking charged particles. Tau lepton identification efficiency is lower than that for electrons or muons, and the fake rate from jets is significant.

In the τjjX final state, one tau lepton must have $E_T > 20 \text{ GeV}$; any other tau leptons must have $E_T > 10 \text{ GeV}$.

TABLE I. Expected Background and Observed Events

	τjjX	di-tau	total
fake taus	5.1 ± 1.3	0.30 ± 0.19	5.4 ± 1.5
$W + \text{jet(s)}$	—	1.3 ± 1.3	1.3 ± 1.3
$Z + \text{jet(s)}$	—	0.6 ± 0.3	0.6 ± 0.3
WW, WZ, ZZ	0.04 ± 0.04	0.04 ± 0.04	0.08 ± 0.06
expected	5.1 ± 1.3	2.2 ± 1.3	7.4 ± 2.0
observed	7	0	7

For the otherwise less stringent di-tau requirements, we raise the E_T requirement to 30 GeV for both tau leptons.

Both final states require $\cancel{E}_T > 30$ GeV. For events in which a jet is mismeasured, the $\vec{\cancel{E}}_T$ typically points toward a jet. To remove much of this background, we require that events satisfy $\Delta\phi/\text{deg} + \cancel{E}_T/\text{GeV} > 60$ where $\Delta\phi$ is the minimum angle in azimuth between an identified object in the event and the $\vec{\cancel{E}}_T$. As events with larger \cancel{E}_T have lower background, this cut becomes less severe as \cancel{E}_T increases.

To reduce contamination from Z boson production, we remove any event that contains a $\mu^+\mu^-$ or e^+e^- pair with an invariant mass between 75 and 105 GeV/ c^2 .

This set of analysis cuts selects 7 events. All pass the τjjX requirements; none passes the di-tau requirements. One event has a tau lepton, an electron, and two jets; the others have a tau lepton and three or more jets. As required, all 7 contain a b -tagged jet.

Data samples and Monte Carlo simulations provide the estimate of the number of expected background events. The expected number of events containing jets which imitate tau leptons is determined from data. Monte Carlo simulations of W and Z plus jet production and diboson (WW , WZ , and ZZ) production are used to determine the largest contributions from processes which produce tau leptons.

Events from QCD and electroweak processes in which a jet mimics a tau lepton dominate the expected background. Unbiased samples of jets allow measurement of the rate (parameterized as a function of jet E_T) at which jets imitate a tau lepton. We replace the normal tau lepton identification cuts with a function that encodes this fake rate and apply it event-by-event to the \cancel{E}_T data sample. This produces a background estimate, 5.4 ± 1.5 , which is absolutely normalized and includes any process contributing to the fake background. In addition to the statistical uncertainty, the quoted uncertainty includes a 25% systematic uncertainty on the measured fake rate. This uncertainty is estimated from differences in the measured fake rates from the various unbiased jet samples.

W and Z plus jets events are generated with the VECBOS Monte Carlo program [17] with an underlying event added by HERWIG [18]. This simulation uses the $\langle p_T^2 \rangle$ of the jets for the QCD renormalization and factoriza-

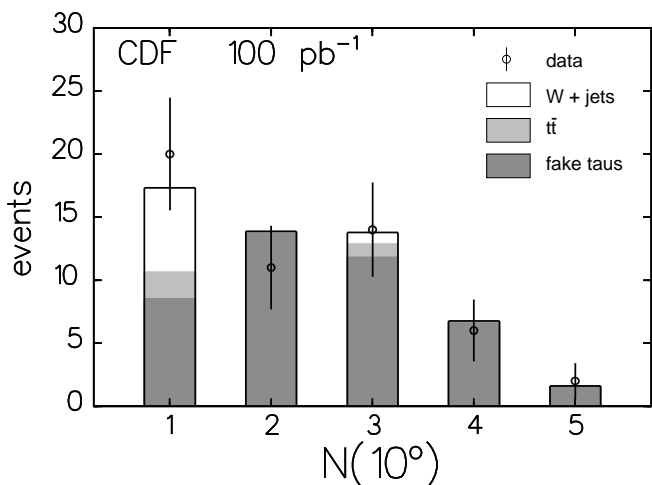


FIG. 1. The charged particle multiplicity (in a 10° cone) of tau candidates ($N(10^\circ)$) in the \cancel{E}_T data sample using cuts that enhance $W \rightarrow \tau\nu + 3$ or more jets events.

tion scales, a minimum p_T of 8 GeV/ c for jets, and the CTEQ3M structure functions [19]. Measured cross sections for $W + \text{jet(s)}$ and $Z + \text{jet(s)}$ production provide the normalization of these Monte Carlo samples [20]. Overall, 1.9 ± 1.3 background events of this type are expected [21].

Diboson production contributes only 0.08 ± 0.06 events to the background expectation. This contribution is determined from an ISAJET 7.06 Monte Carlo [22] which includes tree-level processes for WW , WZ , and ZZ production. Table I shows the number of background events from all sources.

To check the background estimation, we compare the number of observed events without the b -tagging requirement (119) to the total number expected from the various backgrounds (102 ± 21). Moreover, we compare various kinematic distributions (tau E_T , \cancel{E}_T , etc.) both with and without b -tagging to the prediction from the sum of the backgrounds; the agreement is excellent.

To verify that the tau lepton identification algorithm works as expected in events with final states as complex as those from charged Higgs events, a tau signal from $W \rightarrow \tau\nu + 3$ or more jets is selected from the \cancel{E}_T data sample. The cuts for doing this differ slightly from those used for the search. Removing the b -tagging requirement enhances the acceptance, while tightening the \cancel{E}_T requirement to 40 GeV and $\Delta\phi/\text{deg} + \cancel{E}_T/\text{GeV} > 75$ reduces the background in this channel. Figure 1 shows the charged particle multiplicity of tau lepton candidates. (The charge and charged particle multiplicity requirements for the tau lepton are not applied.) The tau signal agrees well with the expectation from W production once backgrounds are taken into account.

Based on an ISAJET Monte Carlo simulation, this analysis would typically retain 2% of the events in which both top quarks decay into H^\pm . Figure 2 shows the ex-

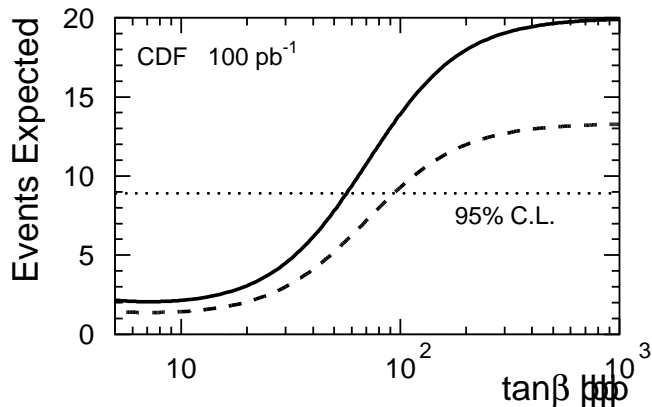


FIG. 2. Expected number of charged Higgs events for $M_{top} = 175 \text{ GeV}/c^2$, $M_{H^\pm} = 100 \text{ GeV}/c^2$, and $\sigma_{t\bar{t}} = 5 \text{ pb}$ (dashed) or 7.5 pb (solid). Models which predict 8.9 or more expected events are excluded at 95% C.L. (dotted).

pected number of signal events as a function of $\tan\beta$ for $M_{top} = 175 \text{ GeV}/c^2$ and $M_{H^\pm} = 100 \text{ GeV}/c^2$. To illustrate the sensitivity to the assumed top cross section $\sigma_{t\bar{t}}$, the figure shows curves for both the theoretical value (5 pb) [23] and another value (7.5 pb) chosen to be 50% above the theoretical expectation. If the two Higgs doublet model is correct, then any measurement of $\sigma_{t\bar{t}}$ that assumes the SM decay $t \rightarrow Wb$ is an underestimate of the true $\sigma_{t\bar{t}}$. The expected contribution to the *signal* when both top quarks decay via the SM mode is 1.35 ± 0.12 events using $\sigma_{t\bar{t}} = 5.0 \text{ pb}$.

The uncertainty in the fake rate measurement (25%) dominates the systematic uncertainty. Varying parameters of the Monte Carlo simulations provides estimates of the systematic uncertainties from the \cancel{E}_T trigger efficiency (10%), from inaccurate modeling of gluon radiation (10%), and from the overall energy calibration of the calorimeter (10%). The uncertainties from tau identification efficiency (10%) and b -tagging efficiency (10%) are determined by comparing Monte Carlo simulations to various data samples. The total systematic error also includes contributions from the integrated luminosity (8%) and limited Monte Carlo statistics at the limit boundary (8%). Adding these contributions in quadrature gives a total systematic uncertainty of 35%.

Using both final states, 7 events are observed and the expected background is 7.4 ± 2.0 events. This analysis excludes at the 95% C.L. any point where the expected number of signal events is 8.9 or larger. The limit calculation includes the relative systematic uncertainties on the background and signal [24].

Figure 3 shows the region excluded by this analysis. For large $\tan\beta$, this analysis excludes charged Higgs bosons with $M_{H^\pm} < 147$ (158) GeV/c^2 for a top quark mass of $175 \text{ GeV}/c^2$ and $\sigma_{t\bar{t}} = 5.0$ (7.5) pb .

The top quark discovery provides additional information which can further restrict H^\pm production. To

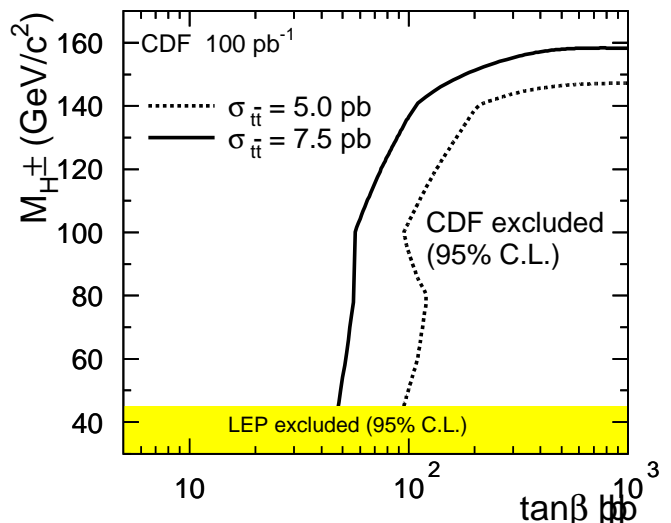


FIG. 3. Charged Higgs exclusion region for $M_{top} = 175 \text{ GeV}/c^2$.

maintain consistency with the observed top cross section $\sigma_0 = 6.8^{+3.6}_{-2.4} \text{ pb}$ [9], $\sigma_{t\bar{t}}$ must increase at higher $\tan\beta$ to compensate for the lower branching fraction into the SM mode $\mathcal{B}(t\bar{t} \rightarrow WbWb)$. Figure 4 shows the region excluded using this additional information.

We thank the Fermilab staff and the technical staffs of the participating institutions for their vital contributions. This work was supported by the U.S. Department of Energy and National Science Foundation; the Italian Istituto Nazionale di Fisica Nucleare; the Ministry of Education, Science and Culture of Japan; the Natural Sciences and Engineering Research Council of Canada; the National Science Council of the Republic of China; the A.P. Sloan Foundation; and the Swiss National Science Foundation.

* Visitor.

- [1] J. Gunion *et al.*, The Higgs Hunter's Guide (Addison-Wesley, New York, 1990); V. Barger, J.L. Hewett, and R.J.N. Phillips, Phys. Rev. D **41**, 3241 (1990); M. Drees and D.P. Roy, Phys. Lett. B **269**, 155 (1991).
- [2] J. Alitti *et al.*, Phys. Lett. B **280**, 137 (1992); C. Albajar *et al.*, Phys. Lett. B **257**, 459 (1991).
- [3] F. Abe *et al.*, Phys. Rev. D **54**, 735 (1996).
- [4] F. Abe *et al.*, Phys. Rev. Lett. **73**, 2667 (1994).
- [5] M.S. Alam *et al.*, Phys. Rev. Lett. **74**, 2885 (1995).
- [6] D. Decamp *et al.*, Phys. Rep. **216**, 254 (1992); P. Abreu *et al.*, Z. Phys. C **64**, 183 (1994); O. Adriani *et al.*, Phys. Lett. B **294**, 457 (1992); G. Alexander *et al.*, *ibid.* **370**, 174 (1996).
- [7] A. Stahl and H. Voss, BONN-HE-96-02 (1996). (to appear in Z. Phys.)

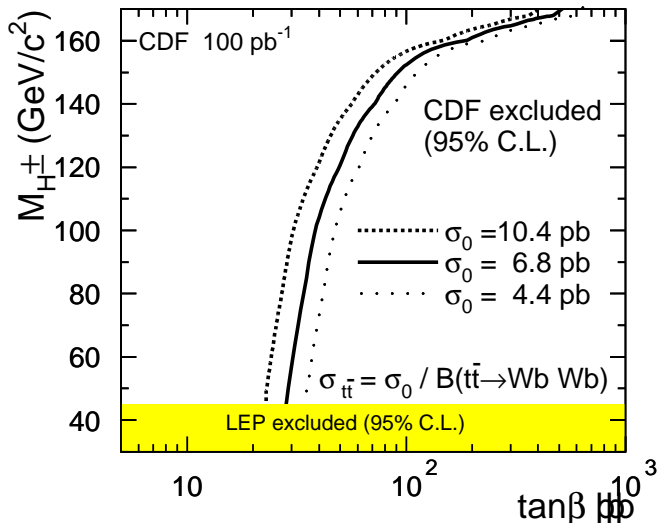


FIG. 4. Charged Higgs exclusion region for $M_{top} = 175$ GeV/c^2 using $\sigma_{t\bar{t}} = \sigma_0 / B(t\bar{t} \rightarrow Wb Wb)$.

- [8] T. Goto and Y. Okada, *Prog. Theor. Phys.* **94**, 407 (1995); F.M. Borzumati and N. Polonsky, *hep-ph/9602433*.
- [9] F. Abe *et al.*, *Phys. Rev. Lett.* **74**, 2626 (1995).
- [10] S. Abachi *et al.*, *Phys. Rev. Lett.* **74**, 2632 (1995).
- [11] F. Abe *et al.*, *Nucl. Instrum. Methods Phys. Res., Sect. A* **271**, 387 (1988).
- [12] The CDF coordinate system defines the polar angle θ with respect to the proton beam direction. The azimuthal angle ϕ is measured in the plane transverse to the beamline. The transverse momentum is defined as $p_T \equiv p \sin \theta$; the transverse energy E_T is similarly defined.
- [13] P. Azzi *et al.*, *Nucl. Instrum. Methods Res., Sect. A* **360**, 137 (1995); D. Amidei *et al.*, *ibid.* **350**, 73 (1994).
- [14] The missing transverse momentum ($\cancel{E}_T \equiv |\vec{\cancel{E}}_T|$) is defined as $\vec{\cancel{E}}_T \equiv -\sum E_T^i \hat{n}_i$ where \hat{n}_i is a unit vector perpendicular to the beamline and pointing at the i th identified physics object (*e.g.*, electron, tau, jet, etc.).
- [15] F. Abe *et al.*, *Phys. Rev. D* **50**, 2966 (1994). See first columns of Tables III and V. Electron fiducial cuts not applied.
- [16] F. Abe *et al.*, *Phys. Rev. D* **45**, 1448 (1992).
- [17] F.A. Berends *et al.*, *Nucl. Phys.* **B357**, 32 (1991).
- [18] G. Marchesini and B.R. Webber, *Nucl. Phys.* **B310**, 461 (1988); *ibid.* **B330**, 261 (1990); I.G. Knowles, *Nucl. Phys.* **B310**, 571 (1988).
- [19] H.L. Lai *et al.*, *Phys. Rev. D* **51**, 4763 (1995).
- [20] F. Abe *et al.*, *Phys. Rev. Lett.* **77**, 448 (1996).
- [21] To avoid double counting background from fake tau leptons, only those Monte Carlo events in which the reconstructed tau lepton matches a generated one within $\Delta R = 0.4$ are used.
- [22] F. Paige and S.D. Protopopescu, Brookhaven National Laboratory Report No. BNL38034, 1986 (unpublished).
- [23] E. Laenen, J. Smith, and W.L. van Neerven, *Phys. Lett. B* **321**, 254 (1994).
- [24] G. Zech, *Nucl. Instrum. Methods Phys. Res., Sect. A* **277**, 608 (1989); T.M. Huber *et al.*, *Phys. Rev. D* **41**,